

# Near-surface gradients of rock quality, deformation modulus, $V_p$ and $Q_p$ to 1 km depth

Nick Barton\*

## Introduction

In hard rock areas, the uppermost 50 m of the ground may consist of soil, weathered jointed rock, and increasingly sound, more massive rock as depth increases. From experience with seismic refraction work, it is well known that there are extreme seismic velocity gradients in this zone. This is so even if we discount the step increase in P-wave velocity,  $V_p$ , at the water table. There are many reasons for the rapid increases in velocity with depth. These include increased stresses, increased rock quality because less weathering has occurred, fewer open joints, less clay, and usually a reduced frequency of jointing.

Besides steep velocity-depth gradients in the top 25m, which are well into double figures when measured in units of  $s^{-1}$ , there are marked increases in the rock mass quality rating  $Q$ , corresponding increases in the rock mass deformation modulus  $E_{mass}$ , and therefore also marked increases in the seismic quality factor for P-waves,  $Q_p$ . Velocity and quality depth gradients generally reduce in steepness beyond some 100-200 m depth, but the correlations between these rock and seismic parameters are reviewed here for depths to 1 km, covering the zone of interest for civil engineering and many mining applications. The importance of these linkages is that the seismic parameters  $V_p$  and  $Q_p$ , which may be determined from seismic refraction and crosshole tomography surveys during site investigation, can be used to estimate the rock mass parameters  $Q$  and  $E_{mass}$  which are needed for engineering design. Applications include excavations in good quality rock, weathered rock, and more porous, weaker rock (Barton, 2006).

In this article, empirical relationships between the rock mass parameters used in engineering design and seismic parameters are presented with reference to the databases

from which they were derived. The first section below introduces the engineers' rock mass parameters. This is followed by separate sections on the linkages between  $V_p$  and rock mass parameters at shallow depths and at greater depths, down to 1 km, and between  $Q_p$  and rock mass parameters. Finally, the relationships are illustrated by a real example.

## Rock mass parameters in engineering

The rock mass quality rating  $Q$  introduced by Barton et al. (1974) is one of the standard international methods of classifying the engineering quality of rock masses, used primarily to assist in the selection of suitable combinations of shotcrete and rock bolts for rock mass reinforcement and support in tunnels and caverns, and to provide input to numerical models. It is determined from surface logging and core logging of the rock mass and has values in the range 0.001 to 1000.

Rock quality  $Q$  is defined as

$$Q = \frac{RQD}{J_n} \times \frac{J_r}{J_a} \times \frac{J_w}{SRF} \quad (1)$$

where RQD is the rock quality designation, defined by the percentage recovery of competent core pieces in lengths >10 cm;  
the value of  $J_n$  depends on the number of joint sets;  
the value of  $J_r$  depends on the joint roughness;  
the value of  $J_a$  depends on the degree of joint alteration and clay filling;  
the value of  $J_w$  depends on the amount of water inflow or pressure; and  
SRF is the stress reduction factor which captures loosening effects due to faulting, and also the stress/strength ratio in the case of massive rock that may fracture under high stress.

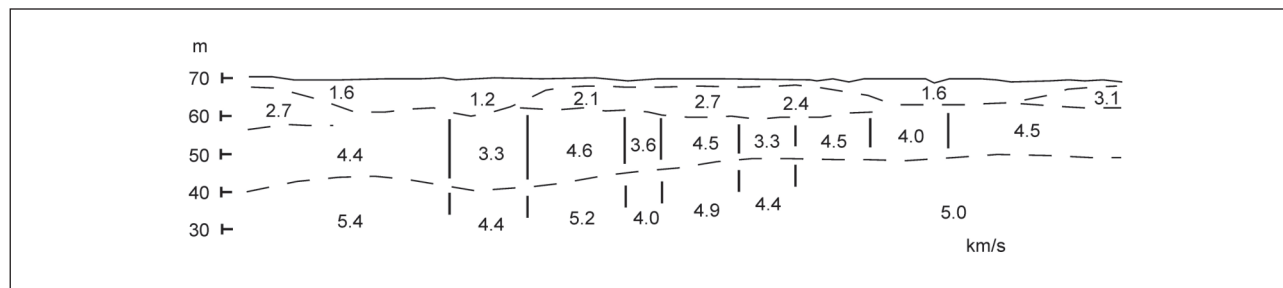


**Figure 1** Example of the steep P-wave velocity gradients seen when conducting shallow seismic refraction at a hard rock, low porosity site in Scandinavia (from Sjøgren, 1984).

\*Fjordveien 65c, 1363, Høvik, Norway; E-mail: nickrbarton@hotmail.com.

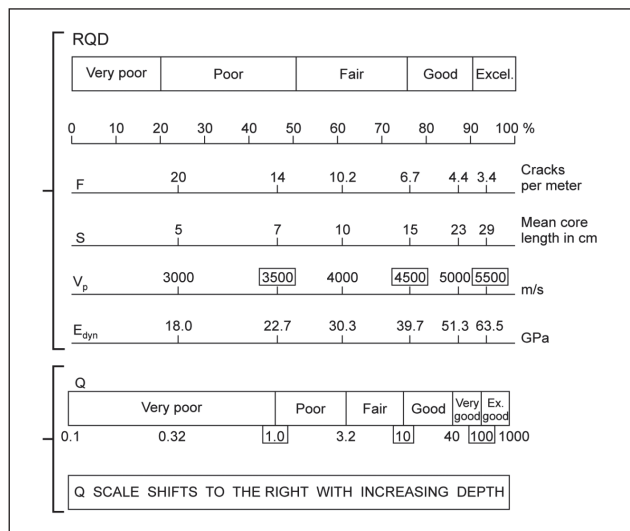


**Figure 2** Mean  $V_p$  and fracture data from recovered core (from Sjøgren et al., 1979). These data were obtained from hard igneous and metamorphic rocks with limited weathering and low porosity. The rock mass quality  $Q$  scales were added by Barton (1995).

Detailed ratings for the six parameters on the right-hand side of equation (1) are too long to be included here, but are tabulated in Barton (2002, 2006). They were developed in the 1970s by exhaustive trial-and-error-fitting to 200 tunnelling case records. In essence, the three pairs of parameter ratios describe block size, inter-block friction, and effective stress, plus the special conditions given by SRF.

For correlation with the parameters  $E_{\text{mass}}$ ,  $V_p$  and  $Q_p$  it is preferable to normalize the rock mass quality rating as  $Q_c$ , defined by

$$Q_c = Q \times \frac{\sigma_c}{100} \quad (2)$$

where  $\sigma_c$  is the uniaxial compressive strength in MPa of core-sized samples, typically 50 mm in diameter. Thus when  $\sigma_c$  has a value of 100 MPa, which is typical of a medium-hard rock,  $Q_c = Q$ . The magnitude of  $Q_c$  shows improved inverse proportionality to permeability in low-porosity rocks where clay is absent.

As developers of the rock mass quality rating  $Q$  (Barton et al., 1974), we had no knowledge of geophysicists' widely used  $Q_p$ , a parameter which is inversely related to attenuation and is approximately independent of frequency over the seismic bandwidth in massive hard rocks. It seems likewise that geophysicists using  $Q_p$  are generally not aware of rock quality  $Q$ . However, these two fundamental rock mass parameters,  $Q$  and  $Q_p$ , prove to be strongly related, as will be demonstrated below.

The rock mass deformation modulus  $E_{\text{mass}}$  is a useful parameter for describing the behaviour of rock masses because it is relatively straightforward to measure directly. It is an important input parameter for numerical modelling of the rock

mass response to excavation.  $E_{\text{mass}}$  is defined as the ratio of normal stress to corresponding normal strain during loading of a rock mass, including elastic and inelastic behaviour, and usually lies in the range from 0.1 to 100 GPa. It is quite distinct from the elastic Young's modulus which is the ratio of normal stress to the normal strain below the elastic limit of the rock.

Laboratory tests on small rock specimens are obviously inappropriate for determining  $E_{\text{mass}}$ , so in-situ tests on large specimens are necessary. Traditionally, the plate-bearing test has been the most commonly used. It involves the application of a load to a rock surface by means of hydraulic jacks or flatjacks, and measurement of the resulting deformation. There are other small-scale types of in-situ tests such as borehole jacking and dilatometer tests that may give higher moduli, which are less relevant for modelling.

In rock engineering, estimates of permeability are required to determine whether grouting of the rock mass is necessary. Permeability is measured in Lugeon units, based on water testing in borehole sections sealed by packers, and in this context is assigned the symbol  $L$ . One Lugeon unit is defined as a water take of 1 litre per minute per metre length of borehole at an excess pressure of 10 bars, and approximately equals a permeability of  $1.3 \times 10^{-7} \text{ m s}^{-1}$  for a porous medium. This is often approximated to  $10^{-7} \text{ m s}^{-1}$  in rock engineering projects. The unit was originally developed for impermeabilization at dam sites, because grouting was judged necessary where the permeability exceeded 1 Lugeon. Lower permeability than this, and therefore high pressure grouting with microcements to reduce inflow, may be required when tunnelling below environmentally sensitive areas. Petroleum geophysicists are more familiar with the Darcy unit for permeability, where 1 Darcy =  $10^{-12} \text{ m}^2$ . In the case of water at 20°C,  $10^{-12} \text{ m}^2$  is equivalent to a rock engineering permeability of  $\sim 10^{-5} \text{ m s}^{-1}$ .

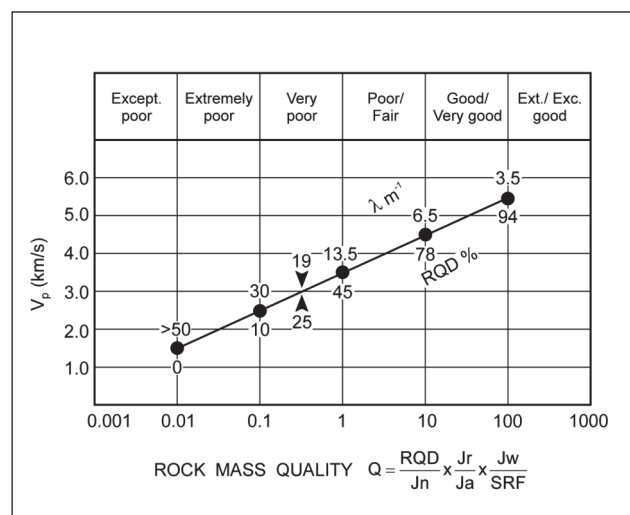


**Figure 3** A synthesis of Fig. 2 corresponding to equation (3), which links  $V_p$  to rock quality  $Q$  in the near-surface.  $\lambda$  (units of  $\text{m}^{-1}$ ) represents crack or joint frequency. Other symbols are defined in the text.

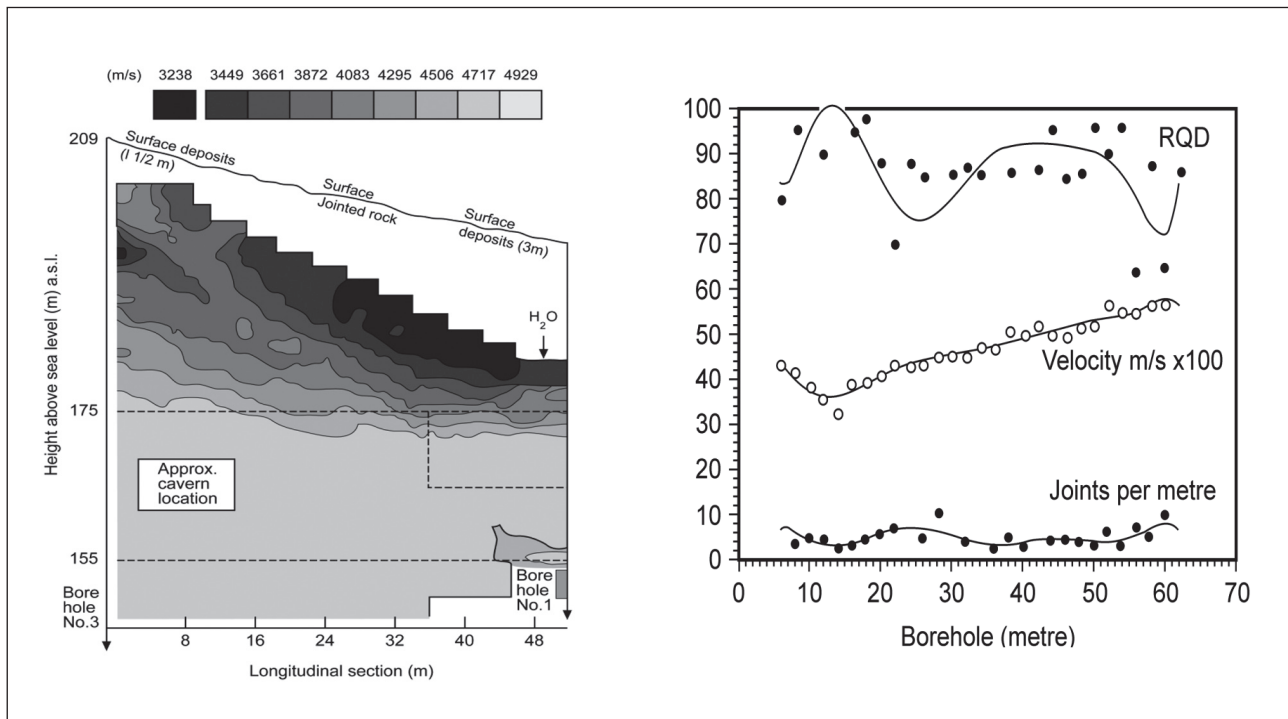


**Figure 4** (a) Cross-hole seismic tomography result showing increasing velocity with depth in jointed gneiss. (b) Velocity, RQD and joint frequency in borehole no. 3, at the left side of the tomographic survey (from Barton et al., 1994).

### Rock quality from seismic velocity at shallow depth

Figure 1 is an interpretation of a shallow seismic refraction profile showing the variation of  $V_p$  with depth (Sjögren, 1984). Clearly there is limited soil cover at this site. Such profiles are typical of pre-construction data for shallow tunnels in hard rock for cases where the depth of weathering is limited.

A particularly useful synthesis of many such near-surface velocity data, interpreted together with local core-logging results, was reported by Sjögren et al. (1979). The mean P-wave velocities and mean core descriptions from 74 drill holes drilled at eight hard rock sites located in Scandinavia, based on 113 km of seismic refraction profiles and 2.9 km of core, are reproduced in Fig. 2. The rocks were mostly granites, gneisses, amphibolites and quartzites with limited weathering and low matrix porosity.

When viewing the shallow seismic-refraction data in Fig. 1, one may pose several questions concerning the implications of increased velocities with depth:

- Do the increased velocities with depth indicate an increase in  $Q$  (or  $Q_c$ )?
- Do the increased velocities indicate an increase in  $Q_p$ ?
- Do the increased stresses with depth affect all the parameters,  $V_p$ ,  $Q$  (or  $Q_c$ ) and  $Q_p$ ?

It may be noted from Figs. 2 and 3, which both apply to shallow hard-rock sites, that a preliminary empirical relationship to link velocity and rock quality in the near-surface is

$$V_p \approx 3.5 + \log Q \quad (3)$$

where the units of  $V_p$  are  $\text{km s}^{-1}$ . This relationship is valid at typical investigation depths for seismic refraction profiles in site investigation, e.g., 20–30 m. Note the convenient increase of 1  $\text{km s}^{-1}$  in  $V_p$  for each ten-fold increase in  $Q$ .

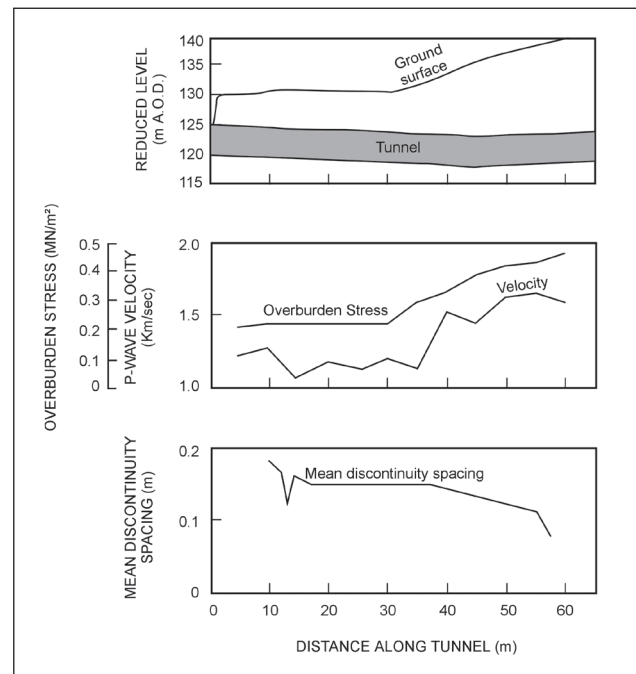


**Figure 5** Example of the effect of depth (or stress) on  $V_p$ . Joint frequency increases at depth, yet velocity continues to rise with overburden stress (from Hudson et al., 1980).

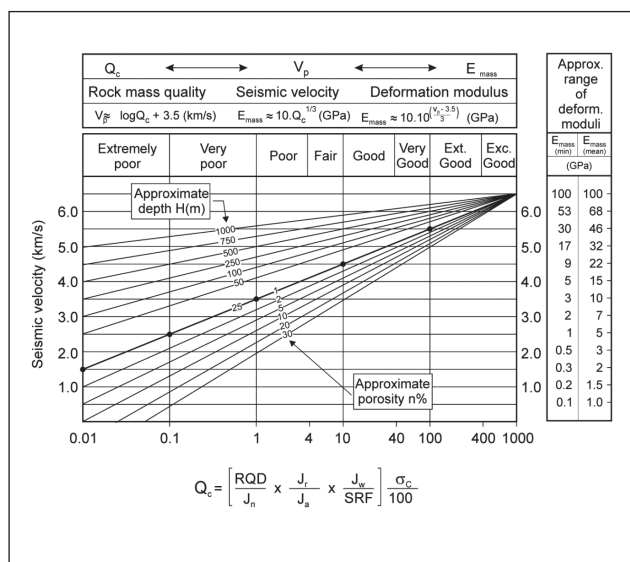


Figure 6 Velocity-depth-porosity- $Q_c$ - $E_{mass}$  correlations, developed from case records and trial-and-error fitting (from Barton, 2006).

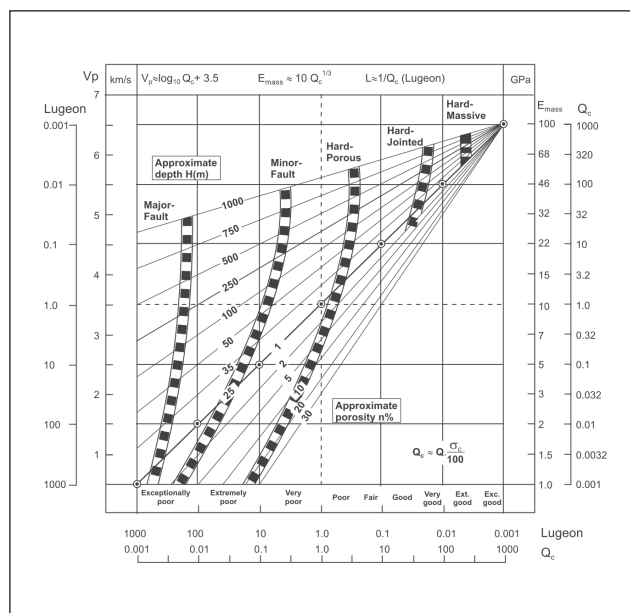


Figure 7 Further development of the correlations in Fig. 6, with the addition of permeability estimation for the case of jointed (but not porous) rock. Type-curves give preliminary indication of the inter-related 'earth-science' properties that can be expected.

In the following section this relationship will be generalized for wider application to weathered rock, to porous rock, and to greater depths. In this extrapolation we will benefit from numerous seismic surveys performed for deep dam foundations, tunnel surveys, and some cross-hole seismic tomography surveys, the deepest to more than 1 km depth. In each case, rock quality variations have also been core-logged, and later shown to correlate with the velocity variations.

## Rock quality from seismic velocity at greater depth

The detailed development of a depth-dependent relationship between  $Q_c$  and  $V_p$  was a process that took several years of trial-and-error, based on analysis of tunnelling sites where detailed personal knowledge of  $Q$  had been obtained from core-logging and where extensive refraction seismic or cross-hole tomography had also been performed. Some of this logging was performed by project colleagues from the Norwegian Geotechnical Institute, Oslo, in boreholes more than 1 km deep, during the nuclear waste disposal site investigations conducted at Sellafield for UK Nirex. A total of 8 km of ignimbrite and tuff were  $Q$ -logged for that project.

A key item in this development was to ascertain the extent to which the velocity  $V_p$  increased with depth in cases where there was no improvement in rock mass quality with depth. Significant examples of this more unusual rock mass condition are shown in Figs. 4 and 5, from an investigation for the 62 m span Gjøvik Olympic cavern in Norway (Barton et al., 1994) and from a research tunnel in jointed chalk at Chinnor in southern England (Hudson et al., 1980).

At the Gjøvik site, crosshole tomography between several pairs of boreholes showed that velocity increases with depth in the jointed gneiss, as expected (Fig. 4a). There was limited weathering and limited soil cover. Closer analysis reveals that the strong velocity increase over the first 50 m (Fig. 4b) is not accompanied by any apparent increase in rock mass quality or decrease in joint frequency over the same interval. The  $Q$ -value ranged between about 5 and 25 ('fair' to 'good' quality) in a similar random manner to RQD and joint frequency, and none of these parameters exhibited any consistent trend with depth. However, permeability did reduce with increased depth, roughly in the range  $10^{-7}$  to  $10^{-8}$  m s $^{-1}$ , presumably due to the joint-closing effects of increased stress.

At Chinnor, an expected velocity increase with overburden depth in chalk is found despite a reduction in the spacing of discontinuities as depth increases (Hudson et al., 1980). This is, of course, an unusual trend, and provides compelling evidence for increase in  $V_p$  with increasing effective stress, despite the reduced rock quality with increased depth. If more clay were present where the discontinuities are more closely spaced, the velocity increase tied to the joint-closing effects of stress increase would be even more marked.

The velocity-depth-porosity- $Q_c$ - $E_{mass}$  chart shown in Fig. 6 was developed over several years of trial-and-error, and also incorporated data obtained from sites in softer rocks such as chalks, chalk marl, sandstones, shales, and some weathered volcanic, igneous, and metamorphic rocks, where both seismic velocities and core-logged  $Q$ -values were available. These more extensive data were obtained from tunnelling and cavern projects in England, Norway, Israel, Hong Kong, and China. The bold diagonal line is directly derived from the mean of the hard rock, shallow seismic refraction data (diagonal line) shown in Fig. 3, partly based on Sjøgren et al. (1979). It has the form



$$V_p \approx 3.5 + \log Q_c \quad (4)$$

where the units of  $V_p$  are  $\text{km s}^{-1}$ , and applies only for low porosity rock at  $\sim 25$  m depth, but now with variable strength. The straight lines above the bold line in Fig. 6 indicate the velocity-rock quality relationships which apply at greater depths. The other straight lines below the bold line give the approximate (-ve) correction for higher porosity rocks. The differences in velocity between these lines for higher porosity and the bold line at constant values of  $Q_c$  are corrections which should be applied for porous rocks at all depths. For example, a hard jointed rock at 500 m depth with  $V_p = 5.0 \text{ km s}^{-1}$  would be expected to have  $Q_c = 1$  if its porosity was 1%, while for the same  $Q_c = 1$ ,  $V_p = 3.5 \text{ km s}^{-1}$  would be expected if its porosity was actually as high as 30%.

The values for the mean rock mass deformation modulus tabulated on the right hand side of Fig. 6 were derived from case records, and show the following empirical relationship (Barton, 1995):

$$E_{\text{mass}} \approx 10 Q_c^{1/3} \quad (5)$$

where the units of  $E_{\text{mass}}$  are GPa. The values of  $E_{\text{mass}}$  used to determine this relationship were obtained from plate-bearing tests or tunnel and shaft deformation analyses. In the latter, multiple position borehole extensometers may be used to give depth-dependent moduli in the excavation disturbed zone, or simple convergence measurement may be used to back-calculate more approximate estimates of  $E_{\text{mass}}$ . The low values of  $E_{\text{mass}}(\text{min})$ , also tabulated, are due to loosening in the excavation disturbed zone that typically surround test sites and tunnelled excavations in rock.

If the input data for  $Q$  (from surface-logging or deeper core-logging) and the uniaxial strength  $\sigma_c$  (from testing in the laboratory) are reliable, equation (5) can be used to give sensible values of  $E_{\text{mass}}$  that are useful for numerical modelling where only a limited number of joints or fractures can be discretely modelled, using their individual stiffnesses. A direct link between velocity and  $E_{\text{mass}}$  that bypasses  $Q$  is also suggested, despite the pseudo-static nature of  $E_{\text{mass}}$ . Depth dependent estimation of  $E_{\text{mass}}$  is therefore possible, and advisable when modelling.

In Fig. 7, the integration of earth-science parameters has been taken a tentative step further, with the inclusion of permeability. As indicated on the scales at the bottom of Fig. 7, the following approximate inverse relationship is proposed:

$$L \approx 1/Q_c \quad (6)$$

where the units of  $L$  are Lugeons. Details of the basis for equation (6) are given in Barton (2006). The central diagonal line and empirical corrections for depth and porosity in Fig. 7 are the same as in Fig. 6. The simplicity and approximate nature of equation (6) is strictly for the case of clay-free rock masses.  $Q_c$  has been refined to a form  $Q_{\text{H}_2\text{O}}$  in Barton

(2006) with inversion of  $J_r/J_a$  to  $J_a/J_r$  in the  $Q$ -rating formula to allow for clay sealing and roughness. There is also a normalized joint wall compression strength (JCS) factor (from Barton and Choubey, 1977) to roughly account for stress-closure effects across the joints or fractures.

The 'type-curves' for 'massive', 'hard jointed', and 'faulted' rock shown in Fig. 7, with their suggested trends of behaviour, will undoubtedly need to be refined where faulting is concerned. An important aspect noted from tunnelling case records (Barton, 2006) is that characterization of fault zones using seismic-tomography performed between pairs of deviated boreholes drilled ahead of the face of deep tunnels, may give a misleading indication of relatively high velocities. This is assumed to be due to the strong compaction of clay within such fault zones.

A fault zone with an 'undisturbed' velocity as high as  $4 \text{ km s}^{-1}$  can nevertheless cause great tunnelling difficulties, leading to collapse or a stuck tunnel boring machine (TBM) cutter-head, due to shearing and de-stressing behaviour as the fault is approached, as if the velocity of the fault zone was much lower, as would be the case closer to the surface.

Here one must also be aware of the 'anomalous' correlation between an optimal tunnelling environment with a low P-wave velocity of  $2\text{--}2.5 \text{ km s}^{-1}$  measured in porous (28%) chalk marl, as in much of the Channel Tunnel between England and France. By contrast, a fault zone in fractured, clay-bearing, and much lower porosity granites, with the same measured velocity of  $2\text{--}2.5 \text{ km s}^{-1}$  when exposed and stress-relieved, may delay tunnelling for many months, such as has occurred many times in Japanese high-speed rail tunnels.

The velocity variations with depth for constant values of  $Q_c$  are shown in a more familiar type of plot in Fig. 8. In real crustal sections, the value of  $Q_c$  increases with depth due to the contrast between the weathered and jointed rock near-surface and the more massive rock commonly found at depth. In effect one experiences 'Q-jumping', which may be gradual or abrupt, both in terms of increased  $Q_c$  and increased  $Q_p$ . Particularly interesting examples are found

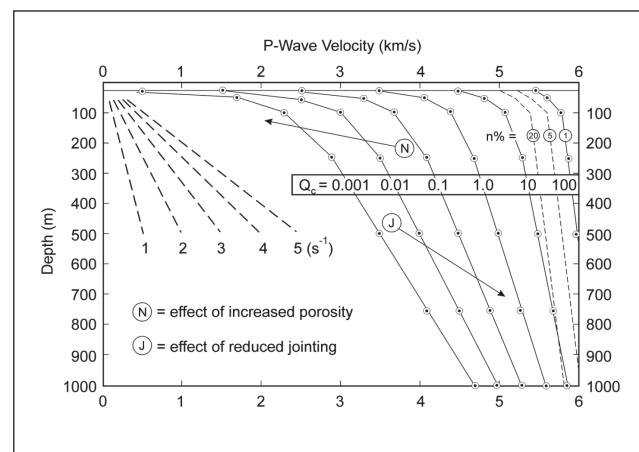
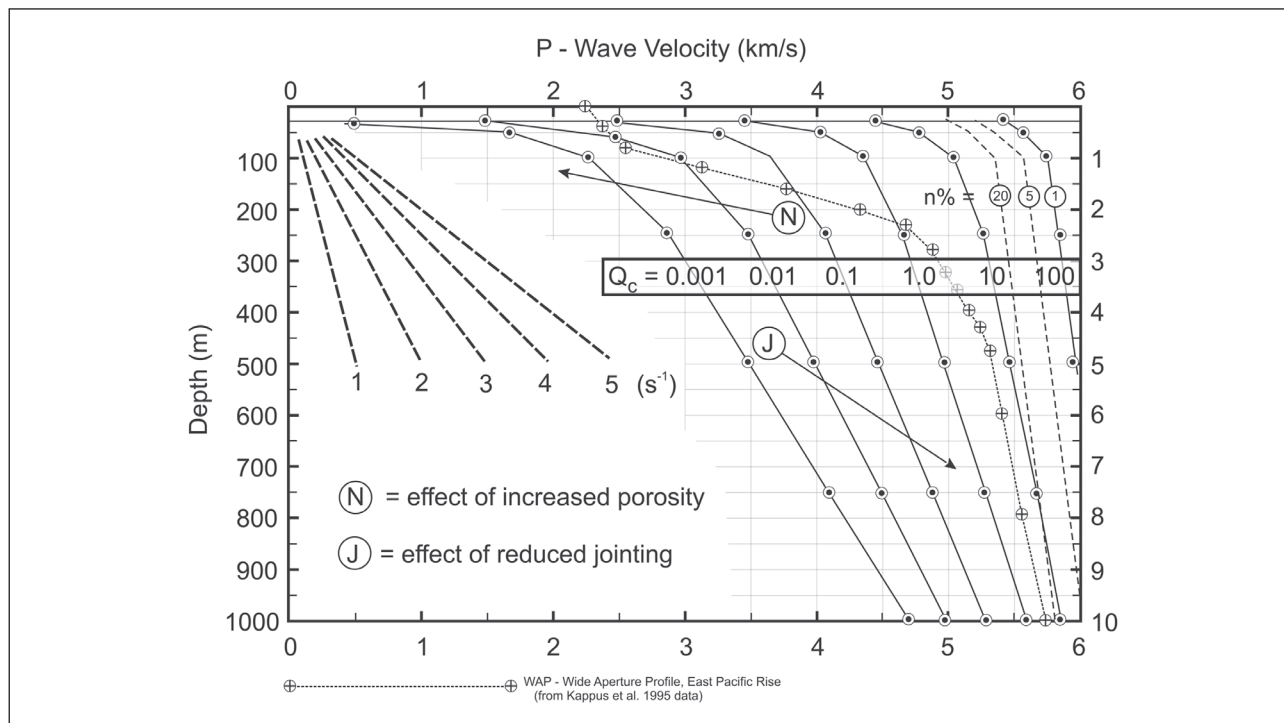


Figure 8 Velocity-depth gradients in familiar form for constant values of rock mass quality rating  $Q_c$ .



**Figure 9** A real example from Kappus et al. (1995) of a velocity-depth profile in mid-ocean ridge basalts is superimposed. Near-sea-floor alteration has given increased porosity, and hydrothermal fluid sealing of the older basalts has stabilized the quality at greater depth. Assumed 'Q-jumping' to successively higher quality rock explains the extra steep velocity-depth gradient. (From Barton, 2006).

in the literature on mid-ocean ridges, where  $Q_c$  presumably increases with depth in essentially the same rock type, based on the measured, greater than expected, increases in  $V_p$ . One example from Kappus et al. (1995) is shown in Fig. 9 and several more are reviewed by Barton (2006).

### Relationship between $Q_p$ and deformation modulus

The results of a very wide ranging literature survey (Barton 2006) suggest that the value of  $Q_p$  can be used to estimate the numerical value of the rock mass deformation modulus  $E_{mass}$  expressed in units of GPa. This possible substitution is shown in Figure 10, and in the following approximation:

$$E_{mass} \approx Q_p \text{ (when } E_{mass} \text{ is in units of GPa)} \quad (7)$$

In the Varian well at Parkfield in California, which is in Tertiary sediments to 1.5 km depth,  $Q_p$  values of 20, 30, and 55 from analysis of depth intervals 0-300 m, 300-940 m, and 570-940 m were reported by Abercrombie (2000) from in-well recordings of earthquakes.  $Q_p$  was found to increase to 110-170 from 1 to 3 km depth. These  $Q_p$  values seem also to be following the likely pattern of pseudo-static deformation moduli, when the latter are expressed in GPa. Such a link may only be intuitive to rock engineers, but it is supported by the remarkable similarities of  $Q_p$  to deformation moduli seen in numerous rock physics test results, when non-linear scales of  $Q_p$  rather than the inverted linear scales of  $1000/Q_p$

or  $Q_p^{-1}$ , are plotted versus effective stress or effective pressure (Barton, 2006).

The actual contributions of scattering and intrinsic loss processes like (micro-) squirt flow and (micro-) friction to  $Q_p$  magnitudes are not of course distinguished in such a simple modulus model, but since estimates of  $E_{mass}$  from  $Q_c$  using equation (5) actually include block size, inter-block friction, the effective stress-to-strength ratio, and water pressure effects, they are in some way sampling variables on which both types of attenuation depend.

Reduced fracture density with depth, reduced friction losses on increasingly stressed fractures, and scattering from a reduced number of fractures, are reported reasons (Abercrombie, 2000) for the increasing  $Q_p$  values with depth. These are all recipes for increased deformation modulus too, and are in accord with the common finding that measured or interpreted values of  $E_{mass}$  in tunnels, vertical shafts and mines increase with depth.

$Q_p$  does not seem to correlate so well with the dynamic modulus  $E_{dyn}$  (Fig. 2) as with the pseudo-static values of  $E_{mass}$  shown in Fig. 6. In principle, the increasing velocity measured at depth, as given on the bottom axis in Fig. 10, takes care of the increasing modulus of deformation with depth. Naturally, at depths of several kilometres, the empirical basis for the above simplicity breaks down, and  $Q_p$  may rise to magnitudes of 500, 1000, and even 5000 at crustal depths. A major review of  $Q_p$ ,  $Q_s$ , and  $Q_{coda}$  is given in Barton (2006)

from rock physics, quarry studies, deep in-well measurements, and earthquake coda analysis.

Prior to excavation, measurements of  $V_p$  may be available from seismic refraction where it is not possible to obtain reliable observations of rock mass quality rating. In these circumstances, combining equations (2), (3), and (5) to eliminate  $Q$ , together with equation (7), yields

$$E_{\text{mass}} \approx Q_p \approx 10^{(V_p - 2.5 + \log \sigma_c) / 3} \quad (8)$$

where  $V_p$  is expressed in units of  $\text{km s}^{-1}$ ,  $E_{\text{mass}}$  in units of GPa and  $\sigma_c$  in units of MPa. This equation, or the nomogram shown in Fig. 10, may be used to estimate  $E_{\text{mass}}$  or  $Q_p$  from measurements of  $V_p$  and  $\sigma_c$  for rock masses in the near-surface. Even though equations (3) and (5) were derived from empirical fits to mostly near-surface data, it is considered reasonable to apply equation (8) and Fig. 10 for a ball-park estimate in the top 1 km of saturated jointed crust, beyond which the empirical database for moduli measurements declines sharply.

### Application example

An example of the application of the above relationships is given here for the South American metro station in granite illustrated in Fig. 11. There are three sets of joints ( $J_n = 9$ ) and weathering is seen in the brown discolouration of many of the joint planes. Many have thin clay fillings ( $J_a = 6$ ) and they are quite planar but with small-scale roughness ( $J_r = 1.5$ ). RQD is quite high at 90-100% (few core pieces < 10 cm length). There is some water (it increases in wet weather) and therefore  $J_w = 0.6$ . Due to the shallow location at 10-20 m depth, SFR = 2.5. The rock matrix is partly weathered, so a lowered uniaxial compressive strength is estimated ( $\sigma = 75$  MPa).

The basic rock mass quality estimation is as follows, using equations (1) and (2):

$$Q_c = \frac{\text{RQD}}{J_n} \times \frac{J_r}{J_a} \times \frac{J_w}{\text{SFR}} \times \frac{\sigma_c}{100} = \frac{90}{9} \times \frac{1.5}{6} \times \frac{0.6}{2.5} \times \frac{75}{100} = 0.5.$$

Equation (4) gives  $V_p \approx 3.2 \text{ km s}^{-1}$ . (Cross-hole velocities in the range 3.0 to 3.5 km/s were typical in the transition to sounder rock between 15-20 m depth at this project).

Equation (5) gives  $E_{\text{mass}} \approx 7.9 \text{ GPa}$ .

Equation (7) gives  $Q_p \approx 8$ .

It may also be noted that equation 6 suggests  $L \approx 2$ , when  $Q_c = 0.5$ , i.e., a permeability of  $2 \times 10^{-7} \text{ m s}^{-1}$ . Grouting was indeed required at this shallow station site, due to numerous permeabilities of similar magnitude. A final stage of Q-system application, if final rock support was also to be chosen for the 18 m span cavern using this method, would be the selection of 14 cm of steel fibre reinforced shotcrete, and systematic bolting at 1.6 m spacing. These quantities are obtained from a Q-system support selection chart (Barton, 2002). In practice an extreme safety factor for metro stations is factored into the effective span (the SPAN/ESR term), and results in an additional final lining of concrete.

At greater depth, say 250 m, and with absence of clay and weathering, a similar-looking rock mass as Figure 11 might show  $Q_c = 15$ . From Fig. 6, we would then see predicted values of  $V_p = 5.5 \text{ km s}^{-1}$  and  $E_{\text{mass}} = 46 \text{ GPa}$ .  $Q_p \approx 46$  (or about 50) is then suggested. From equation (6), permeability might have reduced to approximately  $10^{-8} \text{ m s}^{-1}$ , but a closer estimate to reality would be obtained using  $Q_{\text{H}_2\text{O}}$ , with or without the presence of clay. (Barton 2006).

### Conclusion

There are steep gradients in all the reviewed properties in the near-surface transition through saprolite, weathered jointed rock, and into fresher more massive rock. Quantitative relationships are given here, linking P-wave velocity  $V_p$ , rock mass quality rating  $Q_c$ , rock mass deformation modulus  $E_{\text{mass}}$ , seismic quality factor for P-waves  $Q_p$ , and potentially also permeability  $L$  (when clay is absent), which are applicable for depths to 1 km. These linkages have important applications in site investigation for engineering design for many projects involving excavation and stability of rock masses.

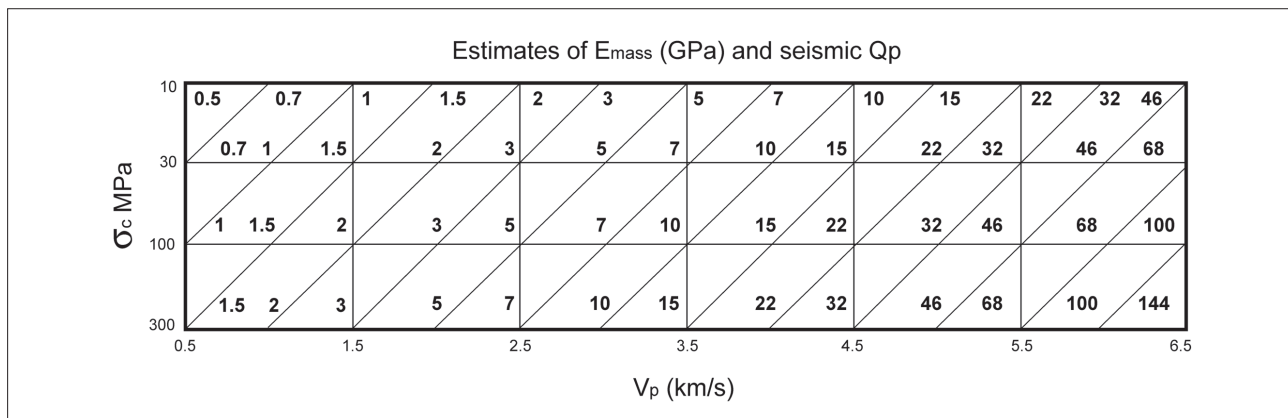


Figure 10 Nomogram relating  $E_{\text{mass}}$  to  $V_p$  and uniaxial strength  $\sigma_c$ . In the first 1 km of jointed rock,  $Q_p$  shows remarkable numerical similarity to  $E_{\text{mass}}$  (with units GPa deleted). See also equation 8.



Figure 11 A shallow excavation in jointed rock for a metro station in South America.

### Acknowledgements

The author wishes to thank the Editor for very helpful suggestions for improving the paper.

### References

- Abercrombie, R.E. [2000] Crustal attenuation and site effects at Parkfield, California. *Journal of Geophysical Research*, **105**, 6277–6286.
- Barton, N., Lien, R. and Lunde, J. [1974] Engineering classification of rock masses for the design of tunnel support. *Rock Mechanics*, **6**, 189–236.
- Barton, N. and Choubey, V. [1977] The shear strength of rock joints in theory and practice. *Rock Mechanics* **1/2**, 1–54.
- Barton, N., By, T.L., Chryssanthakis, P., Tunbridge, L., Kristiansen, J., Løset, F., Bhasin, R.K., Westerdahl, H., and Vik, G. [1994] Predicted and measured performance of the 62m span Norwegian Olympic ice hockey cavern at Gjøvik. *International Journal of Rock Mechanics and Mining Sciences & Geomechanics Abstracts*, **31**, 617–641.
- Barton, N. [1995] The influence of joint properties in modelling jointed rock masses. *Proc. 8th ISRM Congress, Tokyo*, **3**, 1023–1032. Balkema, Rotterdam.
- Barton, N. [2002] Some new Q-value correlations to assist in site characterization and tunnel design. *International Journal of Rock Mechanics and Mining Sciences*, **39**, 185–216.
- Barton, N. [2006] *Rock Quality, Seismic Velocity, Attenuation and Anisotropy*. Taylor & Francis, UK and The Netherlands, 729 pp.
- Hudson, J.A., Jones, E.J.W., and New, B.M. [1980] P-wave velocity measurements in a machine-bored, chalk tunnel. *Quarterly Journal of Engineering Geology*, **13**, 33–43.
- Kappus, M.E., Harding, A.J., and Orcutt, J.A. [1995] A baseline for upper crustal velocity variations along the East Pacific Rise at 13°N. *Journal of Geophysical Research*, **100**, 6143–6161.
- Sjøgren, B. [1984] *Shallow Refraction Seismics*. Chapman and Hall, London.
- Sjøgren, B., Øfsthus, A., and Sandberg, J. [1979] Seismic classification of rock mass qualities. *Geophysical Prospecting*, **27**, 409–442.

**EAGE**  
EUROPEAN  
ASSOCIATION OF  
GEOSCIENTISTS &  
ENGINEERS



**ECMOR X**

**11<sup>th</sup> European Conference on  
the Mathematics of Oil Recovery**

**Call for Papers**  
deadline 5 March 2008  
[www.eage.org](http://www.eage.org)

**8 - 11 September 2008**  
**BERGEN, NORWAY**